Available online at www.sciencedirect.com
ScienceDirect
Journal of Organometallic Chemistry 693 (2008) 483–491
Journal of Organometallic Chemistry
www.elsevier.com/locate/jorganchem

2-(Benzimidazol-2-yl)-1,10-phenanthrolyl metal (Fe and Co) complexes and their catalytic behaviors toward ethylene oligomerization

Min Zhang, Peng Hao, Weiwei Zuo, Suyun Jie, Wen-Hua Sun *

Key Laboratory of Engineering Plastics and Beijing National Laboratory for Molecular Sciences, Institute of Chemistry, Chinese Academy of Sciences, Beijing 100080, China

Received 3 October 2007; received in revised form 8 November 2007; accepted 13 November 2007
Available online 21 November 2007

Abstract

The $N^{\wedge}N^{\wedge}N$-tridentate metal complexes, $LMCl_2$ (M = Fe or Co; L represents a ligand of 2-(benzimidazol-2-yl)-1,10-phenanthrolines), were synthesized and fully characterized with spectroscopic and elemental analysis. The single-crystal X-ray crystallographic analyses revealed complex **1a** with a distorted octahedron geometry due to incorporating one methanol molecule, and complexes **5a** and **9b** with a distorted trigonal-bipyramidal geometry. Upon activation with modified methylaluminoxane (MMAO), these complexes showed good to high catalytic activities toward ethylene oligomerization. The detailed investigations were carried out to disclose the influences of various reaction conditions and nature of ligands on their performing activities of metal complexes.

Keywords: Iron and cobalt tridentate complexes; 2-(Benzimidazol-2-yl)-1,10-phenanthrolines; Ethylene oligomerization

1. Introduction

The major chemical industry of more than 5 million tons of α-olefins provides basic feedstocks for the preparation of detergents, plasticizers and also the comonomers in the copolymerization with ethylene for the linear low-density polyethylene (LLDPE) [1]. The iron and cobalt catalysts showed unique properties for the high selectivity of vinyl-type oligomers and polyolefins (polyolefin waxes) produced, which was initially found by research groups of Brookhart [2] and Gibson [3] using bis(imino)pyridyl iron and cobalt complexes. In the catalytic systems of bis(imino)pyridyl iron and cobalt complexes, more tendency toward ethylene oligomerization was obtained with less steric hindrance of ligands derivatives [4]. In the recent decade, therefore, the intensive researches have explored numerous model complexes of late-transition metals as catalysts toward ethylene reactivity. However, a few models of iron catalysts showed only limited activities [5,6].

Regarding to the coordination environmental requirements of bis(imino)pyridyl iron and cobalt complexes, the $N^{\wedge}N^{\wedge}N$-tridentate ligands would be focused as the core in devising new complexes with potential catalytic activities. During the course of our study, some late-transition metal catalysts have been explored [7]; fortunately, several models of iron and cobalt complexes, ligated by such as derivative ligands of 2-imino-1,10-phenanthrolines (**A**) [8], 2-(2-benzimidazole)-6-iminopyridines (**B**) [9], and 6-(quinoxalin-2-yl)-2-iminopyridines (**C**) [10], showed highly catalytic activities toward ethylene oligomerization and polymerization. 2-(Benzimidazol-2-yl)-1,10-phenanthrolines (**D**) [11], resulted from the incorporation of a benzimidazole group in place of an imino unit of ligands **A**, were designed as ligands in nickel complexes performing high activity toward ethylene dimerization. In parallel, the iron and cobalt complexes containing 2-(benzimidazol-2-yl)-1,10-phenanthrolines have also been synthesized and fully investigated for their catalytic behaviors in ethylene reactivity (see Scheme 1).

* Corresponding author. Tel.: +86 10 62557955; fax: +86 10 62618239.
E-mail address: whsun@iccas.ac.cn (W.-H. Sun).

0022-328X/$ - see front matter © 2007 Elsevier B.V. All rights reserved.
doi:10.1016/j.jorganchem.2007.11.020

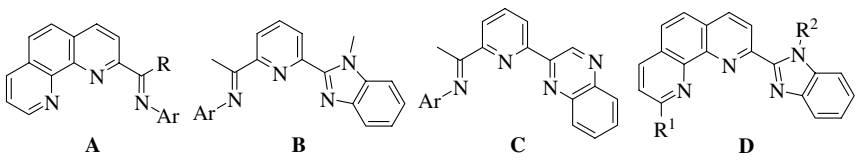

Scheme 1.

The titled iron and cobalt complexes, as a new model of catalysts, showed good catalytic activities toward ethylene oligomerization in the presence of modified methylaluminoxane (MMAO). The influences of catalytic reaction parameters and the steric and electronic effects of ligands were investigated in detail on their catalytic activities and their oligomers obtained. Herein the syntheses and characteristics of those complexes and their catalytic behaviors are reported along with some discussion.

2. Results and discussion

2.1. Synthetic aspects

The tridentate 2-(benzimidazol-2-yl)-1,10-phenanthrolinyl ligands used in this study were prepared via the literature procedures [11]. The iron dichloride complexes **1a**–**10a** were formed by the reaction of an ethanol solution of the corresponding ligand with one equivalent of $FeCl_2 \cdot 4H_2O$ at ambient temperature under nitrogen for 6 h. Following the filtration and washing with cold diethyl ether, the complexes were isolated to give purple powders in good yields (66–82%) with high purity. These complexes are air-stable in the solid state but turned from purple to brown in solution when exposed to air for a few minutes, indicating their oxidation in solution.

The cobalt dichloride complexes **1b**–**10b** could be synthesized in a fashion similar to the corresponding iron complexes. Reactions of these ligands with anhydrous $CoCl_2$ in ethanol at room temperature for 4 h afforded the corresponding complexes **1b**–**10b**, which were isolated in good yields (71–83%). The cobalt complexes are stable in both solution and solid state.

The identity of these iron and cobalt complexes was established by elemental analysis and IR spectrometry. In comparison with the IR spectrometry of free organic compounds [11], the absorption bands of complexes were shifted to lower frequencies, indicating the coordination effects. To understand their real structures, the single crystals of complexes **1a**, **5a** and **9b** were determined by single-crystal X-ray diffraction.

2.2. Molecular structures

Crystals of complexes **1a** and **5a** suitable for X-ray structural determination were obtained by crystallization through the slow layering of diethyl ether onto their methanol solutions. However, single crystals of **9b** were isolated by diffusing the dichloromethane solution with light diethyl ether. Their molecular structures are shown in Figs. 1–3,

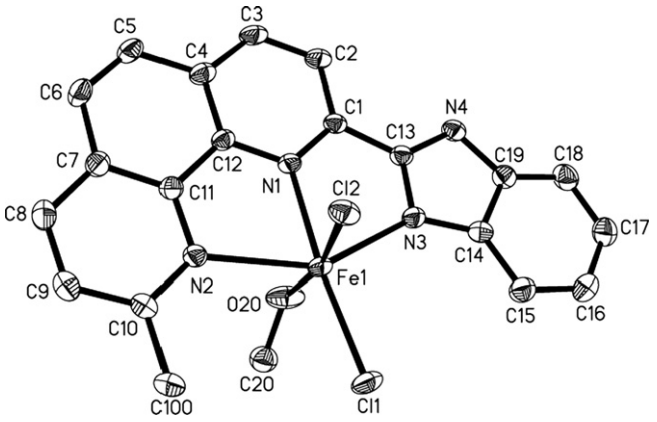

Fig. 1. ORTEP drawing of complex **1a** with thermal ellipsoids at the 30% probability level. Hydrogen atoms have been omitted for clarity.

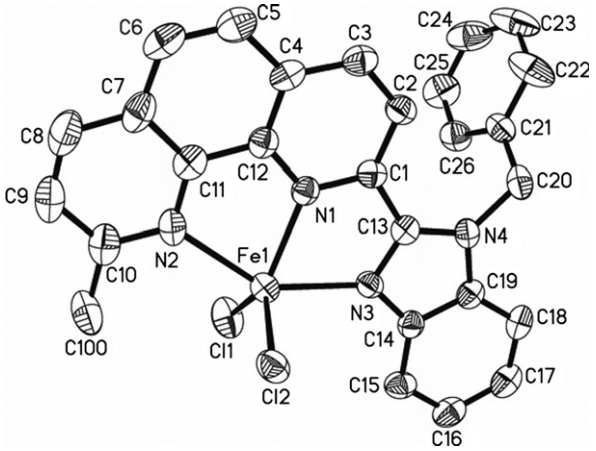

Fig. 2. ORTEP drawing of complex **5a** with thermal ellipsoids at the 30% probability level. Hydrogen atoms have been omitted for clarity.

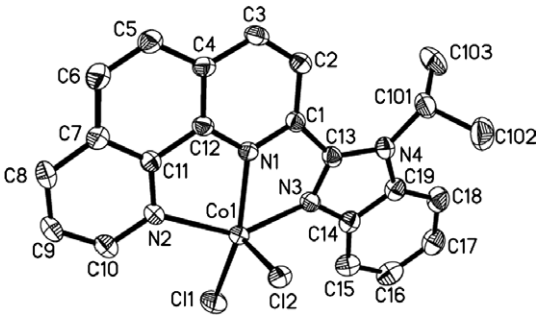

Fig. 3. ORTEP drawing of complex **9b** with thermal ellipsoids at the 30% probability level. Hydrogen atoms and one molecular of CH_2Cl_2 have been omitted for clarity.

Table 1
Selected bond lengths (Å) and angles (°) for complexes **1a**, **5a** and **9b**

	1a (M = Fe)	**5a** (M = Fe)	**9b** (M = Co)
M–N1	2.148(3)	2.117(4)	2.087(4)
M–N2	2.353(3)	2.258(4)	2.167(4)
M–N3	2.232(3)	2.182(4)	2.144(4)
M–Cl1	2.3161(1)	2.2972(2)	2.2634(2)
M–Cl2	2.5889(1)	2.3204(2)	2.3236(2)
N3–C13	1.326(4)	1.329(5)	1.334(6)
N3–C14	1.396(5)	1.382(6)	1.379(7)
N4–C13	1.359(5)	1.366(5)	1.359(6)
N4–C19	1.375(5)	1.402(6)	1.395(7)
N2–M–N1	73.33(1)	74.69(2)	75.97(2)
N2–M–N3	146.81(1)	146.84(2)	144.27(2)
N1–M–N3	73.57(1)	72.90(2)	73.77(2)
N2–M–Cl1	113.85(8)	100.55(1)	98.26(1)
N1–M–Cl1	171.73(9)	129.30(1)	157.83(1)
N3–M–Cl1	99.01(9)	94.53(1)	102.61(1)
N1–M–Cl2	88.46(8)	107.38(1)	92.90(1)
N2–M–Cl2	86.26(8)	95.99(1)	98.31(1)
N3–M–Cl2	95.18(9)	100.13(1)	101.72(1)
Cl1–M–Cl2	95.97(5)	123.26(6)	109.19(6)

individually, and selected bond lengths and angles are listed in Table 1.

In the structure of **1a** (Fig. 1), the coordination geometry around the iron center can be described as a distorted octahedron because of the coordination of the solvent, which is essentially similar to its nickel analogue [11]. As expected, the iron center is coordinated to N1, N2 in the phenanthroline ring and sp^2 hybridized N3 instead of sp^3 N4 in the benzimidazole ring, forming two fused 5-membered rings with acute N–Fe–N angles: 73.33(1)° (N1–Fe1–N2) and 73.57(1)° (N1–Fe1–N3), in which the iron atom lies ca. 0.0666 Å out of the coordinated plane. The benzimidazole plane is nearly oriented coplanar to the phenanthroline plane with a dihedral angle of 4.8°. The bond lengths of Fe–N are significantly different: the Fe1–N1 bond length (2.148(3) Å) is shorter than that of Fe1–N2 (2.353(3) Å) and Fe1–N3 (2.232(3) Å), in which the differences were virtually identical to those seen in the 2,6-bis(imino)pyridyl iron(II) complexes [3] and 2-imino-1,10-phenanthrolinyl iron(II) complexes [8a]. However, there is an unexceptional asymmetry in the two Fe–Cl linkages, with Fe1–Cl(2) being about 0.2728 Å longer than Fe1–Cl(1) in two terminal Cl in *trans*-location, which is much larger than that of its nickel analogue (0.0637 Å) [11].

In the solid state of **5a**, the iron atom is surrounded by a 2-(1-benzyl-benzimidazol-2-yl)-9-methyl-1,10-phenanthroline ligand, and two terminal chlorides. The geometry of the five-coordinate complex can be described as distorted trigonal bipyramidal, with the phenanthroline nitrogen atom (N1) and the two chlorides (Cl1 and Cl2) forming the equatorial plane (Fig. 2). The iron atom slightly deviates by 0.0316 Å from the plane with the equatorial angles between 107.38(1)° and 129.30(1)°, deviating from 120°. The two axial Fe–N bonds subtend an angle of 146.84(2)°, a distortion is a consequence of satisfying the tridentate chelating constraints of the ligand. This equatorial plane is nearly perpendicular to the phenanthrolinyl plane with a dihedral angle of 93.3°. The dihedral angle between bulky benzyl group (R^2) and the phenanthrolinyl plane is nearly perpendicular as 78.0°. It is notable that different R^2 substituents in the ligands have some influence on the Fe1–N3 bond length. The Fe1–N3 bond length of complex **5a** (2.182(4) Å, R^2 = Bn) is shorter than that of complex **1a** (2.232(3) Å, R^2 = H). Similar to complex **1a**, the Fe1–N1(phenanthroline) bond is shorter by about 0.065 Å than Fe1–N3 (benzimidazole) (2.1824 Å) bond and 0.141 Å than Fe1–N2 (phenanthroline) (2.2584 Å) bond, respectively. The two Fe–Cl bond lengths just show a slight difference between the Fe1–Cl2 (2.3204(2) Å) and Fe1–Cl1 (2.2972(2) Å).

As shown in Fig. 3, with the structural features similar to complex **5a**, the cobalt complex **9b** exhibits a distorted trigonal-bipyramidal geometry, with one nitrogen atom (N1) of the phenanthroline and two chlorides composing the equatorial plane. The cobalt atom is almost coplanar with the equatorial plane with the slight deviation of 0.0307 Å. The three equatorial angles N1–Co1–Cl1, N1–Co1–Cl2 and Cl1–Co1–Cl2 are, respectively, 157.83(1)°, 92.90(1)°, and 109.19(6)° whereas the axial Co–N bonds form an angle of 144.27(2)°. The equatorial plane is nearly perpendicular to the phenanthroline plane with a dihedral angle of 93.9°. The two axial Co–N bond lengths, 2.167(4) Å and 2.144(4) Å, are longer than that of Co1–N1 in the equatorial plane, 2.087(4) Å. Furthermore, the two Co–Cl bond distances show a difference of about 0.0602 Å.

2.3. Ethylene oligomerization

The catalytic activity of the novel iron and cobalt precatalysts **1a**–**10a** and **1b**–**10b** presented in Scheme 2 for the oligomerization of ethylene has been evaluated employing modified methylaluminoxane (MMAO) as cocatalyst. The catalysts displayed similar activation characteristics to their analogous nickel systems [11], in which an immediate exotherm was observed without induction period. During the oligomerization reaction (20 min), a decrease in activity was noticed; the final activity was only 5–15% of the initial activity.

Many efforts were devoted to optimizing the catalytic performance. Complexes **6a** and **6b**, the most active precatalysts, were typically scrutinized under a range of reaction conditions (see Tables 2 and 3). The noteworthy results in Tables 2 and 3 disclose some important trends relating reaction parameters to both activity and selectivity for 1-butene. Under optimized conditions, it was observed that ligand environment and metal center have predominant effects on the catalytic properties of the complexes.

2.3.1. Effects of cocatalyst

The precatalysts **6a** and **6b** have been tested in the oligomerization of ethylene with Et_2AlCl, MAO or MMAO as cocatalyst and showed high activities for the dimerization

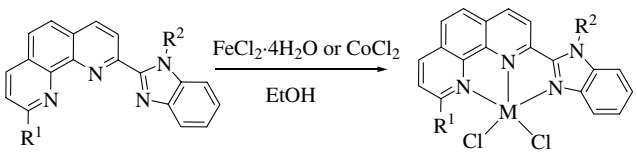

	1a	2a	3a	4a	5a	6a	7a	8a	9a	10a	1b	2b	3b	4b	5b	6b	7b	8b	9b	10b
R^1	Me	Me	Me	Me	Me	H	H	H	H	H	Me	Me	Me	Me	Me	H	H	H	H	H
R^2	H	Me	Et	*i*-Pr	Bn	H	Me	Et	*i*-Pr	Bn	H	Me	Et	*i*-Pr	Bn	H	Me	Et	*i*-Pr	Bn
M	Fe	Fe	Fe	Fe	Fe	Fe	Fe	Fe	Fe	Fe	Co	Co	Co	Co	Co	Co	Co	Co	Co	Co

Scheme 2. Synthesis of tridentate iron and cobalt complexes.

Table 2
Ethylene oligomerization with different cocatalyst[a]

Entry	Complex	Cocatalyst	Al/M	Activity[b]	Oligomer distribution[c] (%)		α-C_4 (%)
					$C_4/\sum C$	$C_6/\sum C$	
1	**6a**	Et_2AlCl	1000	7.27	100		70.3
2	**6a**	MAO	500	10.2	92.7	7.3	91.5
3	**6a**	MAO	800	14.3	93.3	6.7	87.3
4	**6a**	MAO	1000	11.4	96.3	3.7	85.1
5	**6a**	MMAO	1000	35.1	95.0	5.0	92.0
6	**6b**	Et_2AlCl	1000	5.13	98.8	1.2	75.1
7	**6b**	MAO	800	4.22	91.2	8.8	83.8
8	**6b**	MAO	1000	8.03	90.4	9.6	80.1
9	**6b**	MAO	1200	6.20	89.3	10.7	72.5
10	**6b**	MMAO	1000	10.7	88.9	11.1	87.0

[a] General conditions: 5 μmol complex; 100 mL toluene; 20 °C, 30 atm of C_2H_4, 20 min.
[b] 10^5 g mol^{-1} (M) h^{-1}.
[c] Determined by GC.

Table 3
Ethylene oligomerization with **6a**/MMAO and **6b**/MMAO system[a]

Entry	Complex	Al/M	*T* (°C)	*P* (atm)	Activity[b]	Oligomer distribution[c] (%)		α-C_4 (%)
						$C_4/\sum C$	$C_6/\sum C$	
1	**6a**	500	20	30	10.1	97.1	2.9	94.8
2	**6a**	800	20	30	21.7	96.4	3.6	93.5
3	**6a**	1000	20	30	35.1	95.0	5.0	92.0
4	**6a**	1200	20	30	25.3	94.1	5.9	87.2
5	**6a**	1500	20	30	18.1	95.6	4.4	80.1
6	**6a**	1000	40	30	10.6	98.2	1.8	71.8
7	**6a**	1000	60	30	3.10	99.1	0.9	44.0
8	**6a**	1000	80	30	1.43	100		20.1
9	**6a**	1000	20	10	5.72	94.1	5.9	73.8
10	**6a**	1000	20	20	10.2	93.7	6.3	82.6
11	**6b**	500	20	30	4.54	90.5	9.5	88.2
12	**6b**	1000	20	30	10.7	88.9	11.1	87.0
13	**6b**	1200	20	30	15.4	87.4	12.6	84.4
14	**6b**	1500	20	30	23.2	88.2	11.8	83.0
15	**6b**	1800	20	30	13.2	90.1	9.9	78.0
16	**6b**	2000	20	30	10.1	92.0	8.0	75.2
17	**6b**	1500	40	30	9.52	95.1	4.9	60.5
18	**6b**	1500	60	30	4.90	97.7	2.3	33.2
19	**6b**	1500	80	30	1.62	98.5	1.5	23.6
20	**6b**	1500	20	10	3.25	90.4	9.6	68.6
21	**6b**	1500	20	20	9.83	91.3	8.7	77.5

[a] General conditions: 5 μmol complex; 100 mL toluene; 20 min.
[b] 10^5 g mol^{-1} (M) h^{-1}.
[c] Determined by GC.

and trimerization of ethylene (Table 2). The use of different cocatalyst greatly influenced the catalytic results: for both of the complexes **6a** and **6b**, MMAO led to more active and higher selective systems for α-C_4 than Et_2AlCl or MAO (Entries 5 and 10, Table 2). Therefore, further catalytic studies were performed by the activation of MMAO.

2.3.2. Effects of reaction parameters in the presence of MMAO

On the basis of the above preliminary results above, complexes **6a** and **6b** were selected for further optimization, investigating the influence of the [Al]/[M] (M = Fe or Co) molar ratio, reaction temperature and ethylene pressure. The detailed results are shown in Table 3.

The amount of cocatalyst MMAO significantly affected the catalytic results. For iron complex **6a**, the enhancement of Al/Fe molar ratio from 500 to 1000 resulted in an increase of catalytic activity (Entries 1–3, Table 3), which may be attributed to the fact that MMAO scavenged adventitious water and impurities in the solvent at low Al/Fe ratio and the iron complex required more cocatalyst to be activated. With an Al/Fe molar ratio of 1000, the catalytic activity of **6a** peaked at 3.51×10^6 g mol^{-1}(Fe) h^{-1} (Entry 3, Table 3). A further increase of the Al/Fe molar ratio resulted in decreased oligomerization activity (Entries 3–5, Table 3). This observation could be traced to the increasing amount of isobutyl groups which come from MMAO and the generated species hindered the insertion reaction of ethylene due to steric bulkiness [9b,12]. Meanwhile, it is noteworthy that the α-C_4 selectivity of **6a** decreased gradually with the increase of the Al/Fe molar ratio. Therefore, a Al/Fe ratio of 1000 appeared as a good tradeoff between activity and selectivity. For cobalt complex **6b**, the highest activity (2.32×10^6 g mol^{-1}(Co) h^{-1}) was observed at the Al/Co ratio of 1500 (Entry 14, Table 3), and higher or lower amounts of MMAO led to lower activities (Entries 14–16, Table 3). Notably, for both of complexes **6a** and **6b**, the varied amounts of cocatalyst showed no clear impact on the proportion of C_4 component in the products.

As the ethylene oligomerization is a highly exothermic reaction, the reaction temperature significantly affects the catalytic activity. To understand this influence, the two catalytic systems, **6a**/MMAO(Al/Fe = 1000) and

6b/MMAO(Al/Co = 1500) were investigated at 30 atm of ethylene. For the two systems, the elevation of the reaction temperature from 20 °C to 80 °C resulted in a sharp decrease of activity, which may be attributed to the decomposition of the active catalytic sites and lower ethylene solubility at higher temperature (Entries 3, 6–8 and Entries 14, 17–19). Moreover, higher reaction temperature resulted in an increase of the proportion of C_4, but a sharp decrease of selectivity for 1-butene. A similar influence of temperature on the oligomer distribution produced by iron- and cobalt-based systems has been reported [9b].

The studies of pressure variation on ethylene oligomerization by catalysts (**6a** and **6b**) have shown in both cases the ethylene concentration significantly affects the catalytic behavior of the complexes. The increase of ethylene pressure resulted in much higher activities, probably owning to an effect of increased ethylene concentration in solution (Entries 3, 9, 10 and Entries 14, 20, 21). It is also worth mentioning that better selectivity for 1-butene were observed at higher pressure, which can be ascribed to the fact that the increased dimerization activity in turn attenuated the effect of parallel isomerization of 1-butene into 2-butene [13].

2.3.3. Effects of ligand environment and metal center

The results of ethylene oligomerization with all the iron and cobalt complexes as precatalysts are listed in Table 4. It can be observed that the variation of the R^1 and R^2 substituents in the ligands resulted in great changes of the catalytic behaviors, such as activity and α-C_4 selectivity. Similar to the nickel analogues [11], the introduction of a methyl group on the 9-position of the phenanthroline ring led to a decrease in oligomerization activity and a slight increase in α-C_4 selectivity. This could be demonstrated by comparing complexes **1a**–**4a** (R^1 = Me) with **6a**–**9a** (R^1 = H). As shown in Table 4, complexes **6a**–**9a** (Entries 6–9, Table 4) displayed higher activities and lower α-C_4 selectivity than their analogues **1a**–**4a** (Entries 1–4, Table 4). The same trend was also observed for the cobalt dichloride complexes **1b**–**4b**, **6b**–**9b** (compare Entries 16–19 with Entries 11–14, Table 4).

Replacing the active proton on the nitrogen atom of the benzimidazole group in the complex with an alkyl group led to a decrease in oligomerization activity and α-C_4 selectivity. Complexes **1a**, **6a** and **1b**, **6b** containing the N–H group showed much higher activities than their *N*-alkylated analogues (compare Entry 1 with Entries 2–5, Entry 6 with Entries 7–10; Entry 11 with Entries 12–15, Entry 16 with Entries 17–20, Table 4). These results, which concurred with the literature reports [9,14], can be attributed to the deprotonation of the N–H group to give anionic amide ligands when activated by the organoaluminum cocatalyst, and form N–Al species to enhance their catalytic activity. Different alkyl groups, such as methyl, ethyl, isopropyl and benzyl group, showed no obvious influence on α-C_4 selectivity. Meanwhile, the steric bulk effects of these groups on oligomerization activities are not very regular, which may be attributed to the longer distance between the alkyl group and the metal center.

Table 4
Ethylene oligomerization with **1a**–**10a** and **1b**–**10b**/MMAO systems[a]

Entry	Complex	Al/M	Activity[b]	Oligomer distribution[c] (%)		α-C_4 (%)
				$C_4/\sum C$	$C_6/\sum C$	
1	**1a**	1000	10.2	95.6	4.4	95.0
2	**2a**	1000	7.55	92.1	7.9	84.4
3	**3a**	1000	6.23	93.6	6.4	86.0
4	**4a**	1000	6.06	94.6	5.4	85.1
5	**5a**	1000	8.37	94.2	5.8	81.6
6	**6a**	1000	35.1	95.0	5.0	92.0
7	**7a**	1000	10.7	93.2	6.8	82.2
8	**8a**	1000	9.17	95.3	4.7	80.7
9	**9a**	1000	9.22	93.2	6.8	78.4
10	**10a**	1000	7.15	92.9	7.1	75.3
11	**1 b**	1500	10.9	92.1	7.9	91.0
12	**2 b**	1500	7.21	90.3	9.7	83.4
13	**3b**	1500	5.02	90.0	10.0	80.5
14	**4b**	1500	5.52	89.2	10.8	81.7
15	**5b**	1500	7.57	90.2	9.8	77.3
16	**6b**	1500	23.2	88.2	11.8	83.0
17	**7b**	1500	10.4	87.5	12.5	75.0
18	**8b**	1500	8.49	90.1	9.9	74.2
19	**9b**	1500	8.61	91.2	8.8	75.7
20	**10b**	1500	7.02	90.7	9.3	71.2

[a] General conditions: 5 μmol complex; 100 mL toluene; MMAO as cocatalyst; 20 °C, 30 atm of C_2H_4, 20 min.
[b] 10^5 g mol^{-1} (M) h^{-1}.
[c] Determined by GC.

The nature of the metal center has a large influence on catalyst performance. Except for **1a** and **1b**, the activities of the cobalt complexes are substantially lower than for their iron analogues, which keep the trend paralleling the behavior of iron versus cobalt ethylene reactivity catalysts [2,3,8,9b]. Meanwhile, comparison of the oligomerization properties between iron and cobalt catalysts indicated that the cobalt complexes gave a slightly smaller amount of butene and higher amount of hexenes than their corresponding iron complexes. Similar results were also disclosed in 2-arylimino-9-phenyl-1,10-phenanthrolinyl-iron and cobalt complexes [8g]. Compared with the nickel analogues [11], the iron(II) and cobalt(II) complexes containing 2-(benzimidazol-2-yl)-1,10-phenanthroline derivatives showed comparable activities, and as expected, higher selectivity for 1-butene.

3. Conclusions

The synthesis and characterization of a new class of iron- and cobalt-based ethylene oligomerization catalysts ligated by 2-(benzimidazol-2-yl)-1,10-phenanthroline derivatives have been described. On treatment with MMAO, these complexes oligomerize ethylene to dimers and trimers with high activities and good selectivity of α-olefins. This result confirm the hypothesis of $N^{\wedge}N^{\wedge}N$-tridentate iron dihalides potentially having high catalytic activity toward ethylene reactivity. Further experimental results illustrate

their sensitivity toward different ligand environment, Al/M molar ratio, reaction temperature and ethylene pressure. Complexes **1a**–**4a** and **1b**–**4b** with methyl group on the 9-position of the phenanthrolinyl ring ($R^1 = Me$) gave lower activities but higher selectivities for 1-butene than those of complexes **6a**–**9a** and **6b**–**9b** ($R^1 = H$). The incorporation of an alkyl group (R^2) on the N atom of the benzimidazole led to the decrease in oligomerization activity and selectivity for 1-butene (complexes **1a**, **1b**, **6a** and **6b**). In general, higher activities and better selectivity of α-olefin could be obtained under higher ethylene pressure and ambient temperature.

4. Experimental

4.1. General

All air- or moisture-sensitive manipulations were carried out under nitrogen using standard Schlenk techniques. The IR spectra were obtained on a Perkin–Elmer FT-IR 2000 spectrophotometer by using KBr disks in the range of 4000–400 cm^{-1}. Elemental analyses were performed with a Flash EA 1112 microanalyzer. GC was performed with a VARIAN CP-3800 gas chromatograph equipped with a flame ionization detector and a 30 m (0.2 mm i.d., 0.25 μm film thickness) CP-Sil 5 CB column.

Toluene was refluxed in the presence of sodium/benzophenone and distilled under nitrogen prior to use. The polymerization-grade ethylene was supplied by Beijing Yansan Petrochemical Co. Et_2AlCl (1.90 M) solution in toluene was purchased from Acros Chemicals, while methylaluminoxane (MAO, 1.46 M in toluene) and modified methylaluminoxane (MMAO, 1.93 M in heptane, 3A) were purchased from Akzo Nobel Corp. All other commercial chemicals were used without further purification.

4.2. Characterization of complexes *1a–10a* and *1b–10b*

4.2.1. Characterization of complexes *1a–10a*

Characterization data of dichloroiron complexes (**1a**–**10a**). Complex **1a**: purple powder in 80% yield. IR (KBr disk, cm^{-1}): 3250, 3055, 2984, 1623, 1585, 1503, 1427, 1321, 861, 746. Anal. Calc. for $C_{20}H_{14}N_4FeCl_2$ (435.99): C, 54.96; H, 3.23; N, 12.82. Found: C, 54.59; H, 3.42; N, 12.60%. Complex **2a**: purple powder in 72% yield. IR (KBr disk, cm^{-1}): 3047, 2950, 1621, 1585, 1502, 1484, 1465, 857, 741. Anal. Calc. for $C_{21}H_{16}N_4FeCl_2$ (450.01): C, 55.91; H, 3.57; N, 12.42. Found: C, 55.61; H, 3.44; N, 12.17%. Complex **3a**: purple powder in 69% yield. IR (KBr disk, cm^{-1}): 3056, 2954, 1621, 1585, 1489, 1450, 1334, 859, 744. Anal. Calc. for $C_{22}H_{18}N_4FeCl_2$ (464.03): C, 56.81; H, 3.90; N, 12.04. Found: C, 56.55; H, 3.71; N, 12.41%. Complex **4a**: purple powder in 70% yield. IR (KBr disk, cm^{-1}): 3051, 2968, 1620, 1583, 1513, 1453, 1335, 1315, 1163, 867, 743. Anal. Calc. for $C_{23}H_{20}N_4FeCl_2$ (478.04): C, 57.65; H, 4.21; N, 11.69. Found: C, 57.29; H, 4.55; N, 11.29%. Complex **5a**: purple powder in 66% yield. IR (KBr disk, cm^{-1}): 3052, 2961, 1621, 1583, 1519, 1479, 1448, 1429, 1335, 858, 751. Anal. Calc. for $C_{27}H_{20}N_4FeCl_2$ (526.04): C, 61.51; H, 3.82; N, 10.63. Found: C, 61.22; H, 3.51; N, 10.32%. Complex **6a**: purple powder in 77% yield. IR (KBr disk, cm^{-1}): 3281, 3057, 1622, 1579, 1515, 1453, 1323, 862, 747, 703. Anal. Calc. for $C_{19}H_{12}N_4FeCl_2$ (421.98): C, 53.94; H, 2.86; N, 13.24. Found: C, 53.66; H, 2.49; N, 13.61%. Complex **7a**: purple powder in 82% yield. IR (KBr disk, cm^{-1}): 3054, 2942, 1620, 1580, 1528, 1504, 1462, 1415, 1330, 855, 742, 704. Anal. Calc. for $C_{20}H_{14}N_4FeCl_2$ (435.99): C, 54.96; H, 3.23; N, 12.82. Found: C, 54.63; H, 3.01; N, 12.47%. Complex **8a**: purple powder in 79% yield. IR (KBr disk, cm^{-1}): 3058, 2948, 1620, 1606, 1576, 1526, 1483, 1442, 1334, 861, 746. Anal. Calc. for $C_{21}H_{16}N_4FeCl_2$ (450.01): C, 55.91; H, 3.57; N, 12.42. Found: C, 55.52; H, 3.19; N, 12.04%. Complex **9a**: purple powder in 73% yield. IR (KBr disk, cm^{-1}): 3057, 2956, 1626, 1581, 1519, 1439, 1334, 1310, 848, 741. Anal. Calc. for $C_{22}H_{18}N_4FeCl_2$ (464.03): C, 56.81; H, 3.90; N, 12.04. Found: C, 56.47; H, 3.51; N, 12.38%. Complex **10a**: purple powder in 68% yield. IR (KBr disk, cm^{-1}): 3058, 2953, 1622, 1604, 1581, 1526, 1499, 1440, 1334, 851, 737. Anal. Calc. for $C_{26}H_{18}N_4FeCl_2$ (512.03): C, 60.85; H, 3.54; N, 10.92. Found: C, 61.20; H, 3.91; N, 10.66%.

4.2.2. Characterization of complexes *1b–10b*

Characterization data of diclorocobalt complexes (**1b**–**10b**). Complex **1b**: Green powder in 79% yield. IR (KBr disk, cm^{-1}): 3271, 3058, 2964, 1624, 1586, 1503, 1464, 1321, 1148, 863, 745. Anal. Calc. for $C_{20}H_{14}N_4CoCl_2$ (438.99): C, 54.57; H, 3.21; N, 12.73. Found: C, 54.66; H, 3.55; N, 12.38%. Complex **2b**: Green powder in 77% yield. IR (KBr disk, cm^{-1}): 3060, 2947, 1621, 1585, 1524, 1485, 1464, 1335, 1130, 857, 741. Anal. Calc. for $C_{21}H_{16}N_4CoCl_2$ (453.01): C, 55.53; H, 3.55; N, 12.33. Found: C, 55.87; H, 3.19; N, 12.69%. Complex **3b**: Green powder in 80% yield. IR (KBr disk, cm^{-1}): 3061, 2946, 1620, 1583, 1520, 1487, 1448, 1334, 1154, 859, 744. Anal. Calc. for $C_{22}H_{18}N_4CoCl_2$ (467.02): C, 56.43; H, 3.87; N, 11.97. Found: C, 56.81; H, 3.50; N, 12.31%. Complex **4b**: Green powder in 82% yield. IR (KBr disk, cm^{-1}): 3062, 2959, 1620, 1584, 1513, 1455, 1335, 1308, 1162, 867, 743. Anal. Calc. for $C_{23}H_{20}N_4CoCl_2$ (481.04): C, 57.28; H, 4.18; N, 11.62. Found: C, 57.59; H, 4.52; N, 11.27%. Complex **5b**: Green powder in 75% yield. IR (KBr disk, cm^{-1}): 3057, 2960, 1621, 1583, 1520, 1480, 1449, 1335, 1153, 859, 750. Anal. Calc. for $C_{27}H_{20}N_4CoCl_2$ (529.04): C, 61.15; H, 3.80; N, 10.56. Found: C, 61.52; H, 3.45; N, 10.18%. Complex **6b**: Green powder in 71% yield. IR (KBr disk, cm^{-1}): 3283, 3059, 1623, 1576, 1512, 1447, 1321, 1147, 982, 863, 743. Anal. Calc. for $C_{19}H_{12}N_4CoCl_2$ (424.98): C, 53.55; H, 2.84; N, 13.15. Found: C, 53.22; H, 2.51; N, 13.48%. Complex **7b**: Green powder in 76% yield. IR (KBr disk, cm^{-1}): 3057, 2948, 1620, 1574, 1529, 1508, 1459, 1418, 1333, 1131, 848, 741, 704. Anal. Calc. for $C_{20}H_{14}N_4CoCl_2$ (438.99): C, 54.57; H, 3.21; N, 12.73. Found: C, 54.96; H, 3.60; N, 12.37%. Complex **8b**: Green

powder in 77% yield. IR (KBr disk, cm^{-1}): 3061, 2942, 1621, 1608, 1579, 1526, 1483, 1442, 1334, 860, 746. Anal. Calc. for $C_{21}H_{16}N_4CoCl_2$ (453.01): C, 55.53; H, 3.55; N, 12.33. Found: C, 55.80; H, 3.91; N, 12.71%. Complex **9b**: Green powder in 83% yield. IR (KBr disk, cm^{-1}): 3064, 2950, 1622, 1578, 1520, 1439, 1335, 1307, 854, 744. Anal. Calc. for $C_{22}H_{18}N_4CoCl_2$ (467.02): C, 56.43; H, 3.87; N, 11.97. Found: C, 56.74; H, 3.52; N, 11.57%. Complex **10b**: Green powder in 74% yield. IR (KBr disk, cm^{-1}): 3065, 2951, 1621, 1605, 1576, 1524, 1435, 1333, 854, 742, 707. Anal. Calc. for $C_{26}H_{18}N_4CoCl_2$ (515.02): C, 60.49; H, 3.51; N, 10.85. Found: C, 60.77; H, 3.89; N, 11.03%.

4.3. X-ray crystal structure determination of *1a*, *5a* and *9b*

Single-crystal X-ray diffraction studies for complex **1a** and **9b** were carried out on a Rigaku RAXIS Rapid IP diffractometer with graphite-monochromated Mo Kα radiation ($\lambda = 0.71073$ Å). Intensity data for crystals of complex **5a** was collected with a Bruker SMART 1000 CCD diffractometer with graphite-monochromated Mo Kα radiation ($\lambda = 0.71073$ Å). Cell parameters were obtained by global refinement of the positions of all collected reflections. Intensities were corrected for Lorentz and polarization effects and empirical absorption. The structures were solved by direct methods and refined by full-matrix least squares of F^2. All non-hydrogen atoms were refined anisotropically. Structure solution and refinement were performed using the SHELXL-97 Package [15]. Crystal date and processing parameters are summarized in Table 5.

4.4. General procedure for ethylene oligomerization

A 250 mL stainless steel autoclave equipped with a mechanical stirrer and a temperature controller was heated in vacuo at 80 °C for 2 h. It was cooled to the required reaction temperature under ethylene, and charged with toluene, the desired amount of cocatalyst, and toluene solution of catalytic precursor; the total volume was 100 mL.

Table 5
Crystallographic data and refinement for **1a**, **5a** and **9b**

	1a · CH_3OH	**5a**	**9b**
Empirical formula	$C_{21}H_{17}Cl_2FeN_4O$	$C_{27}H_{20}Cl_2FeN_4$	$C_{23}H_{20}Cl_4CoN_4$
f_w	468.14	527.22	553.16
Temperature (K)	296(2)	293(2)	293(2)
Wavelength (Å)	0.71073	0.71073	0.71073
Crystal system	Triclinic	Monoclinic	Monoclinic
Space group	$P\bar{1}$	$P2(1)/c$	$C2/c$
a (Å)	6.9675(1)	12.8396(7)	23.124(5)
b (Å)	11.179(2)	12.8513(8)	12.674(3)
c (Å)	13.640(3)	15.4641(9)	17.258(4)
α (°)	76.77(3)	90	90
β (°)	80.16(3)	72.080(2)	110.56(3)
γ (°)	72.09(3)	90	90
Volume ($Å^3$)	978.3(3)	2427.9(2)	4735.4(2)
Z	2	4	8
D_{calc} ($g\ m^{-3}$)	1.589	1.442	1.552
μ (mm^{-1})	1.065	0.865	1.196
$F(000)$	478	1080	2248
Crystal size (mm)	0.31 × 0.25 × 0.08	0.20 × 0.15 × 0.11	0.32 × 0.15 × 0.13
θ Range (°)	2.70–27.48	2.10–28.31	1.86–27.42
Limiting indicates	$-8 \leqslant h \leqslant 9$, $-14 \leqslant k \leqslant 14$, $-17 \leqslant l \leqslant 17$	$-17 \leqslant h \leqslant 17$, $-17 \leqslant k \leqslant 13$, $-20 \leqslant l \leqslant 20$	$-29 \leqslant h \leqslant 29$, $-16 \leqslant k \leqslant 16$, $-22 \leqslant l \leqslant 22$
No. of reflections collected	6954	24953	10288
No. of unique reflections	4371	5962	5388
R_{int}	0.0414	0.1293	0.0490
Completeness to θ (%)	97.4 ($\theta = 27.48°$)	98.7 ($\theta = 28.31°$)	99.7 ($\theta = 27.42°$)
Absorption coefficient	Empirical	Empirical	Empirical
No. of parameters	271	307	294
Goodness-of-fit on F^2	1.145	0.939	1.071
Final R indices ($I > 2\sigma(I)$)	$R_1 = 0.0572$ $wR_2 = 0.1113$	$R_1 = 0.0603$ $wR_2 = 0.1232$	$R_1 = 0.0670$ $wR_2 = 0.1637$
R indices (all data)	$R_1 = 0.0852$ $wR_2 = 0.1225$	$R_1 = 0.2212$ $wR_2 = 0.1746$	$R_1 = 0.1225$ $wR_2 = 0.1965$
Largest diff peak, hole (e $Å^{-3}$)	0.290, −0.332	0.338, −0.262	0.792, −0.477

The reactor was sealed and pressurized to the desired ethylene pressure, and the ethylene pressure was maintained with feeding of ethylene. After the reaction was carried out for the required period, the pressure was released. A small amount of the reaction solution was collected, and the reaction in this small sample was terminated by the addition of 5% aqueous hydrogen chloride. The organic layer was analyzed by gas chromatography (GC) for determining the composition and mass distribution of oligomers obtained.

5. Supplementary material

CCDC 662797 and 662798 contain the supplementary crystallographic data for this paper. These data can be obtained free of charge from The Cambridge Crystallographic Data Centre via www.ccdc.cam.ac.uk/data_request/cif.

Acknowledgements

This work was supported by NSFC No. 20674089 and MOST No. 2006AA03Z553.

References

[1] (a) D. Vogt, in: B. Cornils, W.A. Herrmann (Eds.), Applied Homogeneous Catalysis with Organometallic Compounds, vol. 1, VCH, Weinheim, Germany, 2002, pp. 240–253;
(b) G.W. Parshall, S.D. Ittel, in: Homogeneous Catalysis: The Applications and Chemistry of Catalysis by Soluble Transition Metal Complexes, Wiley, New York, 1992, pp. 68–72;
(c) J. Skupinska, Chem. Rev. 91 (1991) 613–648.

[2] (a) B.L. Small, M. Brookhart, A.M.A. Bennett, J. Am. Chem. Soc. 120 (1998) 4049–4050;
(b) B.L. Small, M. Brookhart, Macromolecules 32 (1999) 2120–2130.

[3] (a) G.J.P. Britovsek, V.C. Gibson, S.J. McTavish, G.A. Solan, A.J.P. White, D.J. Williams, B.S. Kimberley, P.J. Maddox, Chem. Commun. (1998) 849–850;
(b) G.J.P. Britovsek, S. Mastroianni, G.A. Solan, S.P.D. Baugh, C. Redshaw, V.C. Gibson, A.J.P. White, D.J. Williams, M.R.J. Elsegood, Chem. Eur. J. 6 (2000) 2221–2231.

[4] (a) B.L. Small, M. Brookhart, J. Am. Chem. Soc. 120 (1998) 7143–7144;
(b) G.J.P. Britovsek, M. Bruce, V.C. Gibson, B.S. Kimberley, P.J. Maddox, S. Mastroianni, S.J. McTavish, C. Redshaw, G.A. Solan, S. Strolmberg, A.J.P. White, D.J. Williams, J. Am. Chem. Soc. 121 (1999) 8728–8740;
(c) Z. Ma, W.-H. Sun, N. Zhu, Z. Li, C. Shao, Y. Hu, Polym. Int. 51 (2002) 349–352;
(d) A.S. Abu-Surrah, K. Lappalainen, U. Piironen, P. Lehmus, T. Repo, M. Leskela, J. Organomet. Chem. 648 (2002) 55–61;
(e) C. Bianchini, G. Mantovani, A. Meli, F. Migliacci, F. Zanobini, F. Laschi, A. Sommazzi, Eur. J. Inorg. Chem. (2003) 1620–1631;
(f) M.E. Bluhm, C. Folli, M. Döring, J. Mol. Catal. A: Chem. 212 (2004) 13–18;
(g) I.S. Paulino, U. Schuchardt, J. Mol. Catal. A: Chem. 211 (2004) 55–58.

[5] (a) M. Qian, M. Wang, R. He, J. Mol. Catal. A: Chem. 160 (2000) 243–247;
(b) L. LePichon, D.W. Stephan, X. Gao, Q. Wang, Organometallics 21 (2002) 1362–1366;
(c) C. Bianchini, G. Mantovani, A. Meli, F. Migliacci, F. Laschi, Organometallics 22 (2003) 2545–2547;
(d) M.-S. Zhou, S.-P. Huang, L.-H. Weng, W.-H. Sun, D.-S. Liu, J. Organomet. Chem. 665 (2003) 237–245;
(e) G.J.P. Britovsek, V.C. Gibson, O.D. Hoarau, S.K. Spitzmesser, A.J.P. White, D.J. Williams, Inorg. Chem. 42 (2003) 3454–3465;
(f) R. Cowdell, C.J. Davies, S.J. Hilton, J.-D. Maréchal, G.A. Solan, O. Thomas, J. Fawcett, Dalton Trans. (2004) 3231–3240;
(g) W.-H. Sun, X. Tang, T. Gao, B. Wu, W. Zhang, H. Ma, Organometallics 23 (2004) 5037–5047.

[6] (a) C. Popeney, Z. Guan, Organometallics 24 (2005) 1145–1155;
(b) Q.-Z. Yang, A. Kermagoret, M. Agostinho, O. Siri, P. Braunstein, Organometallics 25 (2006) 5518–5527;
(c) V.C. Gibson, C. Redshaw, G.A. Solan, Chem. Rev. 107 (2007) 1745–1776;
(d) B.L. Small, R. Rios, E.R. Fernandez, M.J. Carney, Organometallics 26 (2007) 1744–1749;
(e) P. Barbaro, C. Bianchini, G. Giambastiani, I.G. Rios, A. Meli, W. Oberhauser, A.M. Segarra, L. Sorace, A. Toti, Organometallics 26 (2007) 4639–4651;
(f) V.C. Gibson, C. Redshaw, G.A. Solan, A.J.P. White, D.J. Williams, Organometallics 26 (2007) 5119–5123;
(g) L. Wang, C. Zhang, Z.-X. Wang, Eur. J. Inorg. Chem. (2007) 2477–2487;
(h) C. Görl, H.G. Alt, J. Organomet. Chem. 692 (2007) 4580–4592.

[7] (a) L. Wang, W.-H. Sun, L. Han, Z. Li, Y. Hu, C. He, C. Yan, J. Organomet. Chem. 650 (2002) 59–64;
(b) W.-H. Sun, W. Zhang, T. Gao, X. Tang, L. Chen, Y. Li, X. Jin, J. Organomet. Chem. 689 (2004) 917–929;
(c) W.-H. Sun, Z. Li, H. Hu, B. Wu, H. Yang, N. Zhu, X. Leng, H. Wang, New J. Chem. 26 (2002) 1474–1478;
(d) C. Shao, W.-H. Sun, Z. Li, Y. Hu, L. Han, Catal. Commun. 3 (2002) 405–410;
(e) S. Jie, D. Zhang, T. Zhang, W.-H. Sun, J. Chen, Q. Ren, D. Liu, G. Zheng, W. Chen, J. Organomet. Chem. 690 (2005) 1739–1749;
(f) J. Hou, W.-H. Sun, S. Zhang, H. Ma, Y. Deng, X. Lu, Organometallics 25 (2006) 236–244;
(g) L. Wang, W.-H. Sun, L. Han, H. Yang, Y. Hu, X. Jin, J. Organomet. Chem. 658 (2002) 62–70;
(h) D. Zhang, S. Jie, T. Zhang, J. Hou, W. Li, D. Zhao, W.-H. Sun, Acta Polym. Sinica. 5 (2004) 758–762;
(i) S. Zhang, I. Vystorop, Z. Tang, W.-H. Sun, Organometallics 26 (2007) 2456–2460;
(j) S. Zhang, W.-H. Sun, X. Kuang, I. Vystorop, J. Yi, J. Organomet. Chem. 692 (2007) 5307–5316;
(k) W.-H. Sun, K. Wang, K. Wedeking, D. Zhang, S. Zhang, J. Cai, Y. Li, Organometallics 26 (2007) 4781–4790.

[8] (a) W.-H. Sun, S. Jie, S. Zhang, W. Zhang, Y. Song, H. Ma, Organometallics 25 (2006) 666–677;
(b) W.-H. Sun, S. Zhang, S. Jie, W. Zhang, Y. Li, H. Ma, J. Chen, K. Wedeking, R. Fröhlich, J. Organomet. Chem. 691 (2006) 4196–4203;
(c) J.D.A. Pelletier, Y.D.M. Champouret, J. Cadarso, L. Clowes, M. Gañete, K. Singh, V. Thanarajasingham, G.A. Solan, J. Organomet. Chem. 691 (2006) 4114–4123;
(d) S. Jie, S. Zhang, K. Wedeking, W. Zhang, H. Ma, X. Lu, Y. Deng, W.-H. Sun, C.R. Chim. 9 (2006) 1500–1509;
(e) S. Jie, S. Zhang, W.-H. Sun, X. Kuang, T. Liu, J. Guo, J. Mol. Catal. A: Chem. 269 (2007) 85–96;
(f) S. Zhang, S. Jie, Q. Shi, W.-H. Sun, J. Guo, J. Mol. Catal. A: Chem. 276 (2007) 174–183;
(g) S. Jie, S. Zhang, W.-H. Sun, Eur. J. Inorg. Chem. (2007) 5584–5598.

[9] (a) P. Hao, S. Zhang, W.-H. Sun, Q. Shi, S. Adewuyi, X. Lu, P. Li, Organometallics 26 (2007) 2439–2446;

(b) W.-H. Sun, P. Hao, S. Zhang, Q. Shi, W. Zuo, X. Tang, Organometallics 26 (2007) 2720–2734.

[10] (a) W.-H. Sun, P. Hao, G. Li, S. Zhang, W. Wang, J. Yi, M. Asma, N. Tang, J. Organomet. Chem. 692 (2007) 4506–4518;
(b) S. Adewuyi, G. Li, S. Zhang, W. Wang, P. Hao, W.-H. Sun, N. Tang, J. Yi, J. Organomet. Chem. 692 (2007) 3532–3541.

[11] M. Zhang, S. Zhang, P. Hao, S. Jie, W.-H. Sun, P. Li, X. Lu, Eur. J. Inorg. Chem. (2007) 3816–3826.

[12] (a) E.Y. Chen, T.J. Marks, Chem. Rev. 100 (2000) 1391–1434;
(b) A.R. Karam, E.L. Catarí, F. López-Linares, G. Agrifoglio, C.L. Albano, A. Díaz-Barrios, T.E. Lehmann, S.V. Pekerar, L.A. Albornoz, R. Atencio, T. González, H.B. Ortega, P. Joskowics, Appl. Catal. A: Gen. 280 (2005) 165–173.

[13] (a) F. Speiser, P. Braunstein, L. Saussine, Organometallics 23 (2004) 2633–2640;
(b) X. Tang, D. Zhang, S. Jie, W.-H. Sun, J. Chen, J. Organomet. Chem. 690 (2005) 3918–3928;
(c) N. Ajellal, M.C.A. Kuhn, A.D.G. Boff, M. Hörner, C.M. Thomas, J.-F. Carpentier, O.L. Casagrande Jr., Organometallics 25 (2006) 1213–1216.

[14] (a) D.S. McGuinness, P. Wasserscheid, D.H. Morgan, J.T. Dixon, Organometallics 24 (2005) 552–556;
(b) W. Zhang, W.-H. Sun, S. Zhang, J. Hou, K. Wedeking, S. Schultz, R. Fröhlich, H. Song, Organometallics 25 (2006) 1961–1969.

[15] G.M. Sheldrick, SHELXTL-97 Program for the Refinement of Crystal Structures, University of Göttingen, Germany, 1997.